[redacted]

Copy 216

RM A56D05

NACA

RESEARCH MEMORANDUM

THE EFFECT OF FLUID INJECTION ON THE COMPRESSIBLE TURBULENT BOUNDARY LAYER - THE EFFECT ON SKIN FRICTION OF AIR INJECTED INTO THE BOUNDARY LAYER OF A CONE AT M = 2.7

By Thorval Tendeland and Arthur F. Okuno

Ames Aeronautical Laboratory
Moffett Field, Calif.

NATIONAL ADVISORY COMMITTEE
FOR AERONAUTICS

WASHINGTON

June 19, 1956

[redacted]

NATIONAL ADVISORY COMMITTEE FOR AERONAUTICS

RESEARCH MEMORANDUM

THE EFFECT OF FLUID INJECTION ON THE COMPRESSIBLE TURBULENT BOUNDARY LAYER - THE EFFECT ON SKIN FRICTION OF AIR INJECTED INTO THE BOUNDARY LAYER OF A CONE AT M = 2.7

By Thorval Tendeland and Arthur F. Okuno

SUMMARY

Data are presented from which the effects of transpiration air flow on average skin-friction coefficients and pressure drag of a conical model were evaluated. The model consisted of a truncated porous cone with a solid ogival nose section. The tests were conducted at a wind-tunnel Mach number of 2.71 and a free-stream Reynolds number range of 6.25×10^6 to 8.56×10^6 per foot. The results of the tests indicated: (1) With a turbulent boundary layer, transpiration air flow results in a reduction of average skin-friction coefficient which is in agreement with the predictions of NACA TN 3341 and the data of NACA RM's A55I19 and A55L13. (2) The use of transpiration air has a destabilizing influence on the laminar boundary layer, tending to cause transition to turbulent flow. (3) No appreciable increase in the pressure drag of the model could be found with transpiration air flow.

INTRODUCTION

One method of cooling the skin of a supersonic aircraft, which shows considerable promise, is transpiration cooling. In a transpiration cooling system, the coolant is forced through the porous skin and out into the boundary layer. Cooling of the aircraft surface occurs as the coolant passes through the pores of the skin and the formation of a protective layer of coolant over the surface tends to decrease the heat-transfer rates to the skin.

References 1 and 2 predict reductions in heat transfer and skin friction with transpiration air flow. For laminar flow, the predictions of heat transfer and skin friction (ref. 3) with transpiration air flow are fairly accurate because the mechanisms of the boundary layer are understood. The theory for turbulent flow, however, is not as reliable

because of the many uncertainties inherent in the analysis. Therefore, there is a definite need for skin-friction and heat-transfer data for turbulent flow in order to substantiate the theoretical predictions and establish relationships for the design of transpiration cooling systems.

Data showing the effects of transpiration air flow on heat transfer for turbulent flow have been reported in reference 4 and the limited skin-friction data available for turbulent flow are analyzed in reference 5. Considerable effort has been made at Ames Aeronautical Laboratory to obtain skin-friction data with transpiration air flow by the momentum-loss method from impact-pressure surveys of the boundary layer but this method has inherent inaccuracies.

Therefore, the present tests were made to determine the effects of transpiration air flow on skin friction by means of measurements of drag forces, surface pressures, and base pressures. The model was a truncated porous cone with a solid ogival nose. The tests were conducted at a nominal tunnel Mach number of 2.71 and over a Reynolds number range of 6.25×10^6 to 8.56×10^6 per foot. Turbulent flow was obtained by use of a boundary-layer trip on the model.

SYMBOLS

C_F average skin-friction coefficient, dimensionless

C_f local skin-friction coefficient, dimensionless

D_F skin-friction drag, lb

F dimensionless mass-flow rate normal to surface, $\frac{\rho_w v_w}{\rho_1 u_1}$

q dynamic pressure, lb/sq ft

R Reynolds number, dimensionless

R_1 Reynolds number based on model length and average velocity over the surface, dimensionless

S surface area, sq ft

p static pressure, lb/sq ft

ρ density of air, lb/cu ft

u velocity component parallel to surface, ft/sec

v velocity component normal to surface, ft/sec

x coordinate along model center line measured from the tip, in.

Subscripts

o zero injection condition

w condition at surface

∞ undisturbed free-stream condition

1 outer edge of boundary layer

DESCRIPTION OF EQUIPMENT

The tests were conducted in the Ames 6-inch heat-transfer wind tunnel. A description of the wind tunnel is given in reference 6. The wind tunnel pressure level may be varied to obtain data over a range in Reynolds number at a nominal Mach number of 2.71.

A diagrammatic sketch of the model as installed for testing is shown in figure 1. The model consisted of a truncated porous cone to which was attached an ogival shaped nose with a fineness ratio of 2.43. The ogival shaped nose section was used in order to reduce the model length and thus to permit testing without interference from the nose shock wave after it was reflected from the tunnel walls.

The porous cone section was obtained commercially. This section was hollow and was fabricated from many layers of fine copper wire wrapped in a suitable pattern. These layers were bonded together by means of a sintering process. The porous section was not a perfectly straight conical section but had a small surface curvature which caused the cone angle to vary near the small diameter of the section. This nonsymmetry of the cone angle extended over a length of approximately 2 inches. The total included angle of the porous section was approximately 10°.

As shown in figure 1, the model was supported by means of a strain-gage balance assembly. The strain-gage balance was used to measure drag forces. The strain-gage assembly and other equipment were enclosed by the support fairing at the base of the model. This fairing could be adjusted axially to permit any gap desired between the fairing and the base of the model. Enclosed within the fairing and near the base of the model was a tube for measuring base pressures. Dry injection air entered

the model by means of a spiral wound flexible connection. With this spiral connection, the thrust from the transpiration air did not affect the drag force measurements; also, any restraints from the tubing used to bring the transpiration air into the model could not be detected with the strain-gage balance. The transpiration air entered the model at approximately room temperature and was controlled by means of a suitable valve. Flow rates were measured with rotameters.

Twelve pressure taps were installed to measure pressures along the surface of the model. Three of the taps were located on the nose section and the other nine on the porous section. Two of the pressure taps on the nose section were installed opposite from one another and thus enabled the adjustment of the model to zero angle of attack. In order to obtain turbulent flow over the model, a boundary-layer trip was used. The trip consisted of a 3/16-inch-wide strip of 5/0 garnet paper and was located 9/32 inch from the tip. Four static-pressure taps, spaced along the tunnel side wall, were used in conjunction with the stagnation pressure to evaluate the free-stream Mach number.

TEST PROCEDURE

The first portion of the test program consisted of measuring drag forces and base pressures for various tunnel conditions and for various transpiration air-flow rates. The strain gage used to measure drag forces was calibrated before the model was placed in the tunnel. A check of the calibration was made before or after each tunnel run. Data were obtained both with and without a boundary-layer trip.

Upon completion of the drag-force measurements, the surface-pressure taps were connected to a dibutylphthylate manometer and surface pressures were measured for the same tunnel conditions and the same transpiration air-flow rates as were used in the drag-force tests. During all tests, steady-state conditions of temperature and pressure were obtained before taking any data.

REDUCTION OF DATA

Drag Data

Pressure drag was evaluated as the product of the average pressure which acted on the model in the direction of the air stream and the frontal area of the model. The average pressure which acted in the direction of the air stream was obtained by plotting measured surface pressures versus frontal area. This plot was then integrated to determine an average pressure. To obtain a continuous curve of surface pressures along the

model, the value at the tip was determined from conical-shock values given in reference 7. The surface pressure measurement nearest the base of the model was not used. This pressure measurement was believed to be inaccurate due to a slight recess of the pressure tap with respect to the surface of the model.

The scatter or differences when pressure drag was measured from two or more sets of data were approximately ±1/2 of 1 percent. It is believed that this difference is representative of the error in measuring and reducing the data in order to obtain an average value of pressure with respect to the frontal area of the model.

Base-pressure drag was determined as the product of the base pressure and the base area of the model. Drag forces were evaluated from the measurements obtained with the strain-gage balance. With regard to the strain-gage measurements, a zero shift in the strain-gage calibration was encountered. To adjust for this zero shift, gage zeros were taken at the beginning and at the end of each run and small adjustments were made to the strain-gage measurements.

Average Skin-Friction Coefficients

The skin-friction drag of the model was determined by subtracting the pressure drag from the sum of the base-pressure drag and the force drag measurements. Since only the skin-friction drag of the porous section is of interest, this drag was determined by subtracting the calculated skin-friction drag of the ogival nose section from the total skin-friction drag of the model. Average skin-friction coefficient for the porous section was evaluated by the method described in the appendix.

Experimental Error

The experimental error in evaluating an average skin-friction coefficient is believed to be due mainly to the error in determining an average surface pressure and also the error in force measurement as a result of the zero shift in strain-gage calibration. A small uncertainty of approximately ±1 percent also exists with regard to calculating the skin-friction drag of the solid nose section. As pointed out previously, the uncertainty in determining an average surface pressure was approximately ±1/2 of 1 percent. However, since the pressure drag was approximately 10 times the skin-friction drag, this error results in an uncertainty of approximately ±5 percent in determining an average skin-friction coefficient. The zero shifts in the strain-gage calibration caused an

uncertainty in the force measurements of ±2 percent. Therefore, since the errors as mentioned are additive, the total estimated experimental uncertainty in determining average skin-friction coefficients is ±8 percent.

The drag of the boundary-layer trip is believed to be of smaller magnitude than the accuracy of the drag force measurements. The basis for this conclusion was that two trips of different thicknesses were tried and no drag associated with the trips could be detected. The trip thicknesses used were 0.007 and 0.009 inch and were obtained by using 5/0 garnet paper with different backing thicknesses.

DISCUSSION OF RESULTS

Pressure Distribution

Typical values of surface-pressure-ratio distribution along the model are shown in figure 2 for one Reynolds number and both with and without transpiration air flow. The surface-pressure ratios on the solid ogival nose were the same with or without transpiration air flow. It can be seen from figure 2 that the effect of transpiration air flow on the pressure-ratio distribution is to increase the pressure ratio near the beginning of the porous section (values of x from 2-1/2 to 4-1/2 inches), while near the base of the model there is a slight decrease in the measured pressure ratio. This increase in surface pressure is canceled by a decrease which follows when an average pressure is determined with respect to the frontal area of the model. The reason the smaller pressure difference cancels the larger pressure difference is that an average pressure is determined by integrating measured surface pressures with respect to frontal area, and the frontal area per unit length is greater near the base of the model than near the nose. Therefore, within the experimental accuracy of the tests no difference in pressure drag was found with the use of transpiration air.

Base Pressure Drag

The base pressures measured in these tests do not conform to those for a body simply supported by a rod or a small sting. In these tests a fairing was used at the base of the model to enclose the strain-gage balance and other accessory equipment. This fairing matched the contour of the cone section and was adjusted so that the gap between the fairing and the base of the model was approximately 0.010 inch to 0.015 inch. The pressures as measured at the base of the model were sensitive to this gap width and therefore they are not indicative of what could be expected on a body with a blunt unshielded base.

Average Skin-Friction Coefficients

Experimental values of average skin-friction coefficients for the porous section of the model are shown in figure 3. These values were obtained with no transpiration air flow. For comparison, theoretical values of average skin-friction coefficients for the porous section are also shown. These values were calculated by the method given in the appendix. The experimental skin-friction coefficients are somewhat higher than the calculated values. This is probably due to the fact that the surface of the porous section was not smooth but had a surface irregularity or roughness as a result of the method used to fabricate the porous material. The effect of surface roughness on skin-friction coefficient is believed to be similar to that reported in reference 8. The effect of Reynolds number on the experimental skin-friction coefficients is not apparent because of the small Reynolds number range over which the data were obtained.

Effects of Transpiration Air

The effect of transpiration air flow on turbulent skin-friction coefficients are shown in figure 4. In this figure the ratio of C_F/C_{F_o} versus F is shown for several free-stream Reynolds numbers. These values are for the porous section of the model. The solid-line curves in figure 4 were faired through the data to indicate the trend of the data.

An inspection of figure 4 shows the reduction in skin-friction coefficient with transpiration air flow is large. For example, for a value of F of 0.002, a reduction of approximately 40 percent in average skin-friction coefficient occurs. Whether any of this reduction in skin friction occurred because the body was not perfectly smooth is not known. The data in figure 4 show no particular effect of Reynolds number. However, as determined analytically the effect of Reynolds number for the range of test conditions is small.

The effect of transpiration air flow without a boundary-layer trip on the model is shown in figure 5. In this figure, values of C_F versus F are shown without a boundary-layer trip on the model. For comparison, values are also shown when a boundary-layer trip was used to obtain turbulent flow. With no boundary-layer trip and at a low Reynolds number, the increase in skin friction at the low rates of transpiration air flow is very apparent. This increase was probably due to the transition point of the boundary layer moving upstream with the use of transpiration air and thereby causing the flow over a greater portion of the cone surface to be turbulent. With a further increase in the transpiration air-flow rate, a decrease in the turbulent skin-friction coefficient results. Shadowgraph

pictures of the model showed that transition moved upstream with an increase in transpiration air-flow rates. It is interesting to note that the skin-friction coefficient obtained at the same Reynolds number and both with and without a boundary-layer trip are approximately equal at the higher transpiration air-flow rates. This indicates that the effect of the start of turbulent flow near the model tip as compared to the beginning of the porous section was small. This effect was calculated and found to be less than 13 percent. A difference of this magnitude could not be detected because of the scatter of the data. The agreement of the data obtained with and without a boundary-layer trip substantiates the conclusion that the drag of the trip was within the accuracy of the tests.

In figure 5, the skin-friction coefficients at a Reynolds number per foot of 4.28×10^6 are higher than the skin-friction coefficients at a Reynolds number per foot of 6.25×10^6 for values of F above 0.0008. Computations from the theory of reference 1 indicate that the difference in skin-friction coefficients is a Reynolds number effect which increases with increasing transpiration air flow.

Comparison With Theory

In order to obtain a comparison of the measured reductions in skin-friction coefficients with theoretical predictions, the data obtained in this experiment are compared in figure 6 to theoretical curves calculated by the methods given in references 1 and 2. In this figure values of C_F/C_{F_o} are plotted versus $2F/C_{F_o}$. For an additional comparison, four data points, two from reference 4 and two from reference 5, are also shown in figure 6. The two data points from reference 4 are average values of a number of data points which were obtained by means of heat-transfer measurements on a flat plate. These data were converted to equivalent local skin-friction values by the method given in reference 1. The data from reference 5 were obtained from a flat plate by calculating the momentum thickness from impact-pressure surveys in the boundary layer at several stations along the plate. Local skin-friction coefficient was determined from the difference between the local momentum-thickness gradient and local injection parameter.

An inspection of figure 6 shows that the reductions in average skin-friction coefficients as determined from these tests are in reasonable agreement with the theoretical curve calculated by the method given in reference 1. The theory of reference 2, however, predicts a larger decrease in skin friction with the use of transpiration air than was found in these tests. A comparison of the data in these tests with that obtained from references 4 and 5 is good considering the fact that the data were obtained from three different models and by means of three different experimental techniques.

In figure 6 the skin-friction coefficients for the theoretical curves and the data from references 4 and 5 are local values for a flat plate. These values are compared to the average skin-friction coefficients obtained from a conical surface in these tests. This comparison is possible because the relationship between the local values for C_f/C_{f_o} and $2F/C_{f_o}$ for a flat plate is the same as the relationship between the average values for C_F/C_{F_o} and $2F/C_{F_o}$; also, the relationship between average values for C_F/C_{F_o} and $2F/C_{F_o}$ for a cone and a flat plate is the same.

As mentioned previously, it is not known what the effect of surface roughness was on the reduction in skin-friction coefficient with transpiration air flow. However, the agreement of the data in these tests with those obtained from references 4 and 5 certainly indicates that surface roughness did not have a major effect on the reduction in skin-friction coefficient with transpiration air flow.

As shown in reference 1, transpiration air injection with turbulent flow results in practically the same reduction in both Stanton number and skin-friction coefficient. Therefore, reductions in heat-transfer coefficients comparable to the reductions in skin-friction coefficients shown in figures 4 and 5 would be expected to result from the use of transpiration air flow.

CONCLUSIONS

Wind-tunnel tests were conducted to determine the effects of transpiration air flow on the skin-friction and pressure drag of a conical model. Data were obtained at a nominal tunnel Mach number of 2.71 and free-stream Reynolds numbers of 6.25×10^6 to 8.56×10^6 per foot. The pertinent results may be summarized as follows:

1. Transpiration air flow results in a reduction of average skin-friction coefficient for turbulent flow which is in agreement with the predictions of NACA TN 3341 and the data of RM's A55I19 and A55L13.

2. The use of transpiration air has a destabilizing influence on the laminar boundary layer, tending to cause transition to turbulent flow.

3. No appreciable increase in the pressure drag of the model could be found over the range of transpiration air-flow rates used in the test.

Ames Aeronautical Laboratory
National Advisory Committee for Aeronautics
Moffett Field, Calif., Apr. 5, 1956

[redacted]

APPENDIX

The skin-friction drag of the nose section was evaluated by calculation of local skin-friction coefficients for various stations along the nose section and integration of these local values with respect to the surface area in order to obtain average skin-friction coefficients. The drag of the nose section was then evaluated by means of the equation

$$C_F = \frac{D_F}{q_1 S}$$

where $q_1 S$ was taken as the average value over the nose. Local skin-friction coefficients were evaluated as follows:

1. Laminar flow was assumed to exist up to the boundary-layer trip, and with no trip, laminar flow was assumed to exist over the entire nose section. This assumption was substantiated by means of shadowgraph pictures. Local laminar skin-friction coefficients were calculated by means of the correlation of reference 9, which is that local skin-friction coefficients for cones at zero angle of attack are equal to the $\sqrt{3}$ times the corresponding coefficients for flat plates under identical local free-stream conditions. Local flat-plate skin-friction coefficients were determined by means of the results given in reference 10.

2. Beyond the boundary-layer trip, the turbulent skin-friction coefficients were calculated using the rule given in reference 11. This rule is that the local heat transfer for a cone is the same as for a flat plate at one half the local Reynolds number on the cone, the Mach number and wall-to-free-stream temperature remaining the same. Since heat transfer and skin friction are proportional, this rule also applies to local skin-friction coefficients for cones. Local flat-plate skin-friction coefficients for turbulent flow were calculated by the T' method given in reference 12.

To calculate the local skin-friction coefficients it was necessary to resort to an estimate of the effective start of turbulent flow in order to determine the local Reynolds number. However, the effect of this estimate on the skin-friction drag of the nose section and the subsequent skin-friction drag of the porous section is indicated as follows: The skin-friction drag of the nose section was approximately 15 percent of the skin-friction drag of the porous section. Therefore, an error of 10 percent in the skin-friction drag of the nose section would result in an error of less than 2 percent in the skin-friction drag of the porous section. For comparison, calculations of skin-friction drag for the nose section were made on the assumption that the start of turbulent flow began at the tip of the model and also that turbulent flow started halfway between the tip

and the boundary-layer trip. The calculated values agreed within 5 percent. Therefore, since the location of the start of turbulent flow did not appreciably affect the skin-friction drag of the porous section, all of the calculations for skin-friction coefficients were made on the assumption that turbulent flow began at the tip of the model. Local conditions of flow at the outer edge of the boundary layer and lengths along the test surface were used to calculate local skin-friction coefficients. The method used to calculate the average skin-friction coefficients for the nose section was also used to calculate the average skin-friction coefficients for the porous section which are shown in figure 3.

[redacted]

REFERENCES

1. Rubesin, Morris W.: An Analytical Estimation of the Effect of Transpiration Cooling on the Heat-Transfer and Skin-Friction Characteristics of a Compressible, Turbulent Boundary Layer. NACA TN 3341, 1954.

2. Dorrance, William H., and Dore, Frank J.: The Effect of Mass Transfer on the Compressible Turbulent Boundary Layer Skin Friction and Heat Transfer. Rep. No. ZA-7-013, Consolidated Vultee Aircraft Corp., San Diego, Calif., Aug. 5, 1954.

3. Brown, W. Byron, and Donoughe, Patrick L.: Tables of Exact Laminar-Boundary-Layer Solutions When the Wall is Porous and Fluid Properties are Variable. NACA TN 2479, 1951.

4. Rubesin, Morris W., Pappas, Constantine C., and Okuno, Arthur F.: The Effect of Fluid Injection On the Compressible Turbulent Boundary Layer - Preliminary Tests on Transpiration Cooling of a Flat Plate at M = 2.7 With Air as the Injected Gas. NACA RM A55I19, 1955.

5. Rubesin, Morris W.: The Influence of Surface Injection on Heat Transfer and Skin Friction Associated With the High-Speed Turbulent Boundary Layer. NACA RM A55L13, 1956.

6. Stalder, Jackson R., Rubesin, Morris W., and Tendeland, Thorval: A Determination of the Laminar-, Transitional-, and Turbulent-Boundary-Layer Temperature-Recovery Factors on a Flat Plate in Supersonic Flow. NACA TN 2077, 1950.

7. Ames Research Staff: Equations, Tables, and Charts for Compressible Flow. NACA Rep. 1135, 1953.

8. Czarnecki, K. R., Robinson, Ross B., and Hilton, John H., Jr.: Investigation of Distributed Surface Roughness on a Body of Revolution at a Mach Number of 1.61. NACA TN 3230, 1954.

9. Hantzsche, W., and Wendt, H.: The Laminar Boundary Layer of a Circular Cone in Supersonic Flow at Zero Angle of Attack. Jahrbuch der Deutschen Luftfahrtforschung, 1941, p.I, pp. 76-77. (Also available as: (1) British Ministry of Supply, Volkenrode, MOS 115 (V 487) (Rep. and Trans. 276) Aug., 1946; (2) Univ. of Calif., Eng. Res. Projects Trans., May 1, 1947.)

10. Van Driest, E. R.: Investigation of Laminar Boundary Layer in Compressible Fluids Using the Crocco Method. NACA TN 2597, 1952.

11. Van Driest, E. R.: Turbulent Boundary Layer on a Cone in a Supersonic Flow at Zero Angle of Attack. Jour. Aero. Sci., vol. 19, Jan. 1952, pp. 55-57, 72.

12. Sommer, Simon C., and Short, Barbara J.: Free-Flight Measurements of Turbulent-Boundary-Layer Skin Friction in the Presence of Severe Aerodynamic Heating at Mach Numbers From 2.8 to 7.0. NACA TN 3391, 1955.

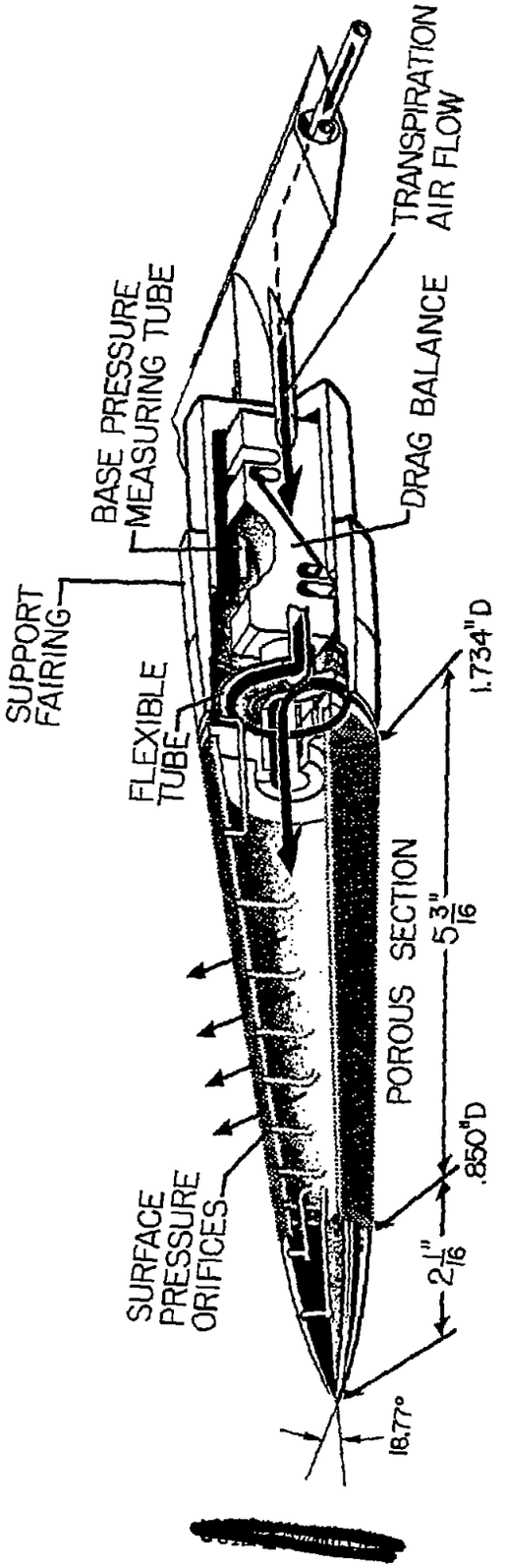

Figure 1.- A diagrammatic sketch of the model assembled for testing.

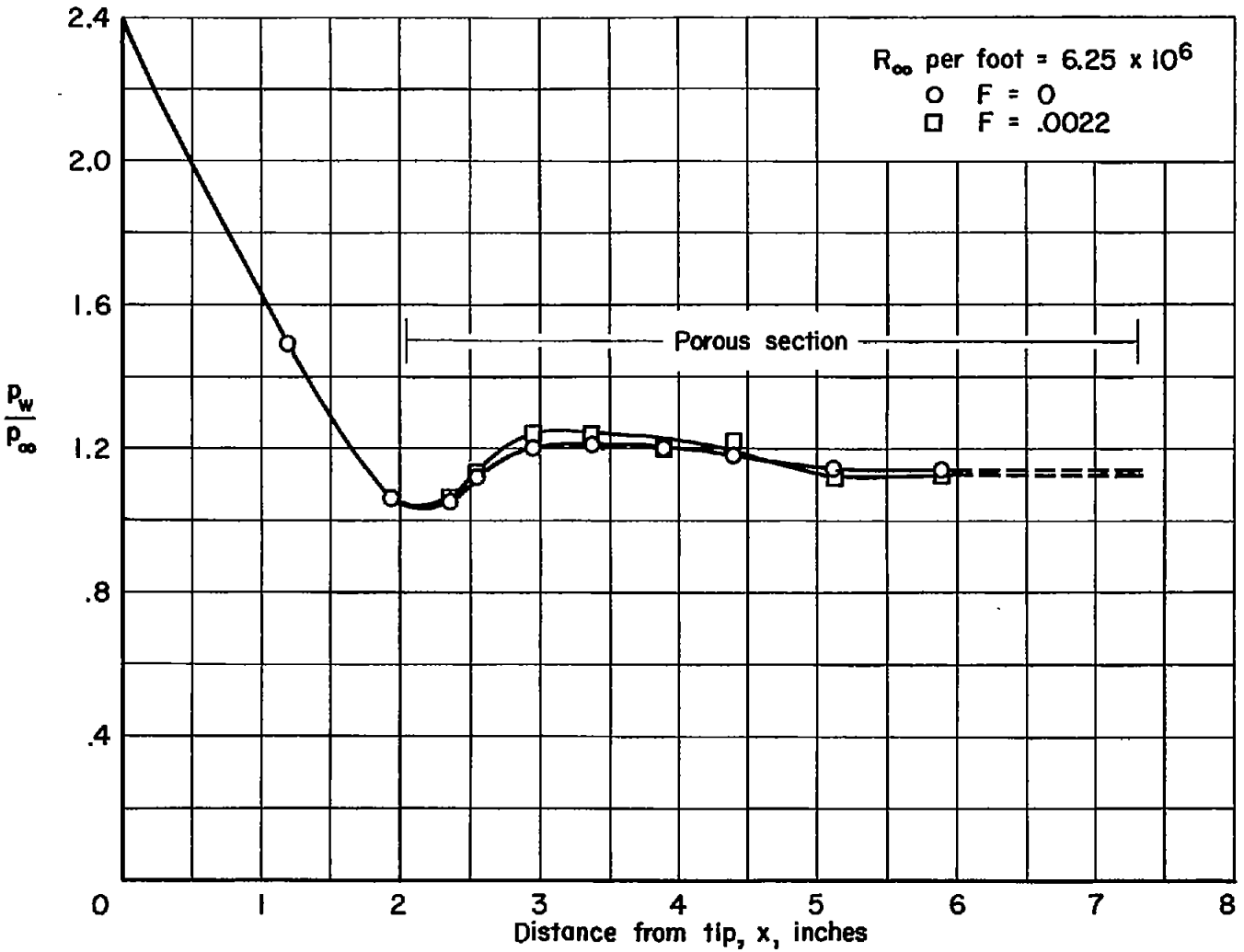

Figure 2.- Typical pressure distributions, both with and without transpiration air flow.

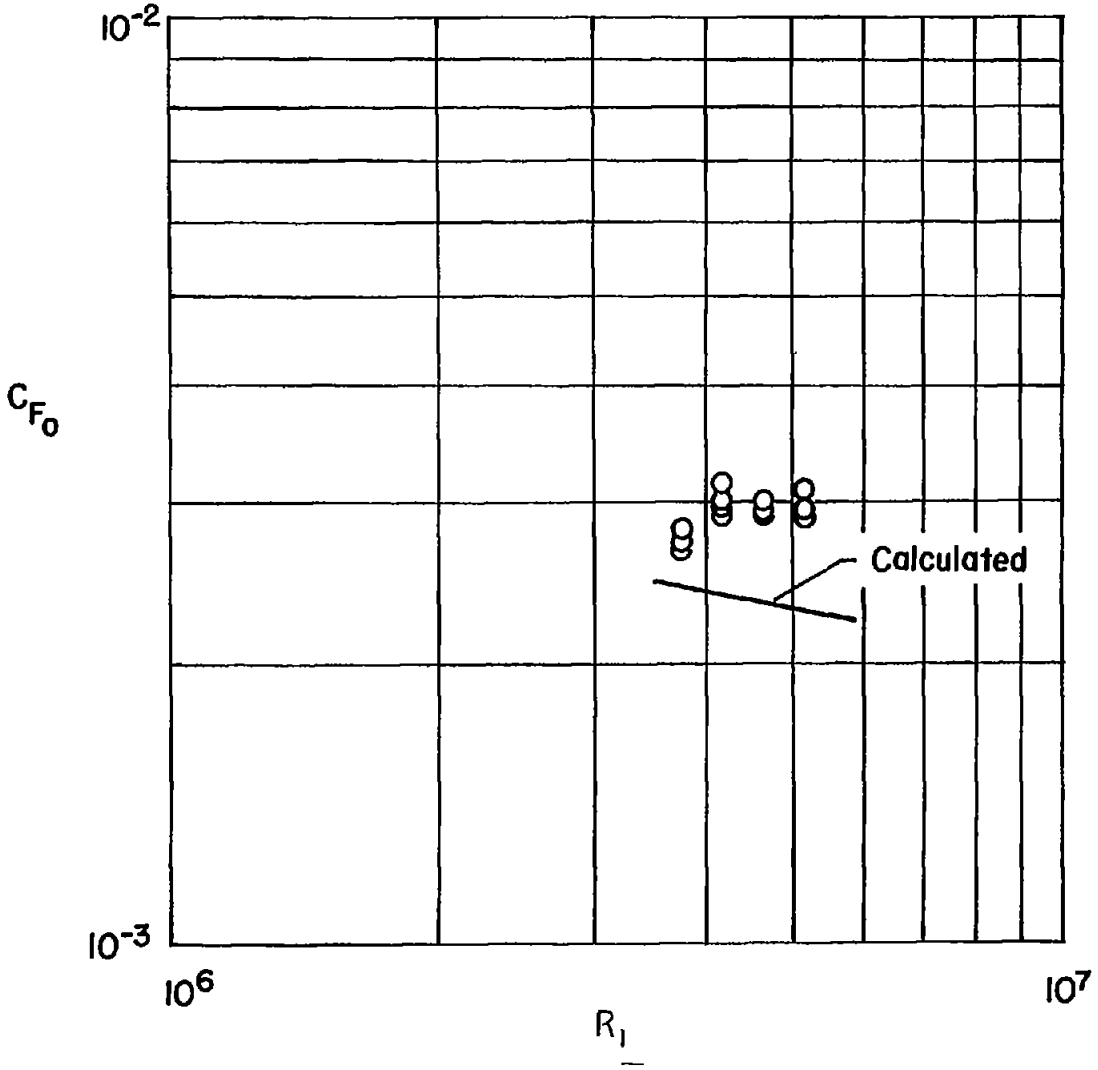

Figure 3.- Comparison of experimental skin friction with calculated values for the porous section; no transpiration air flow.

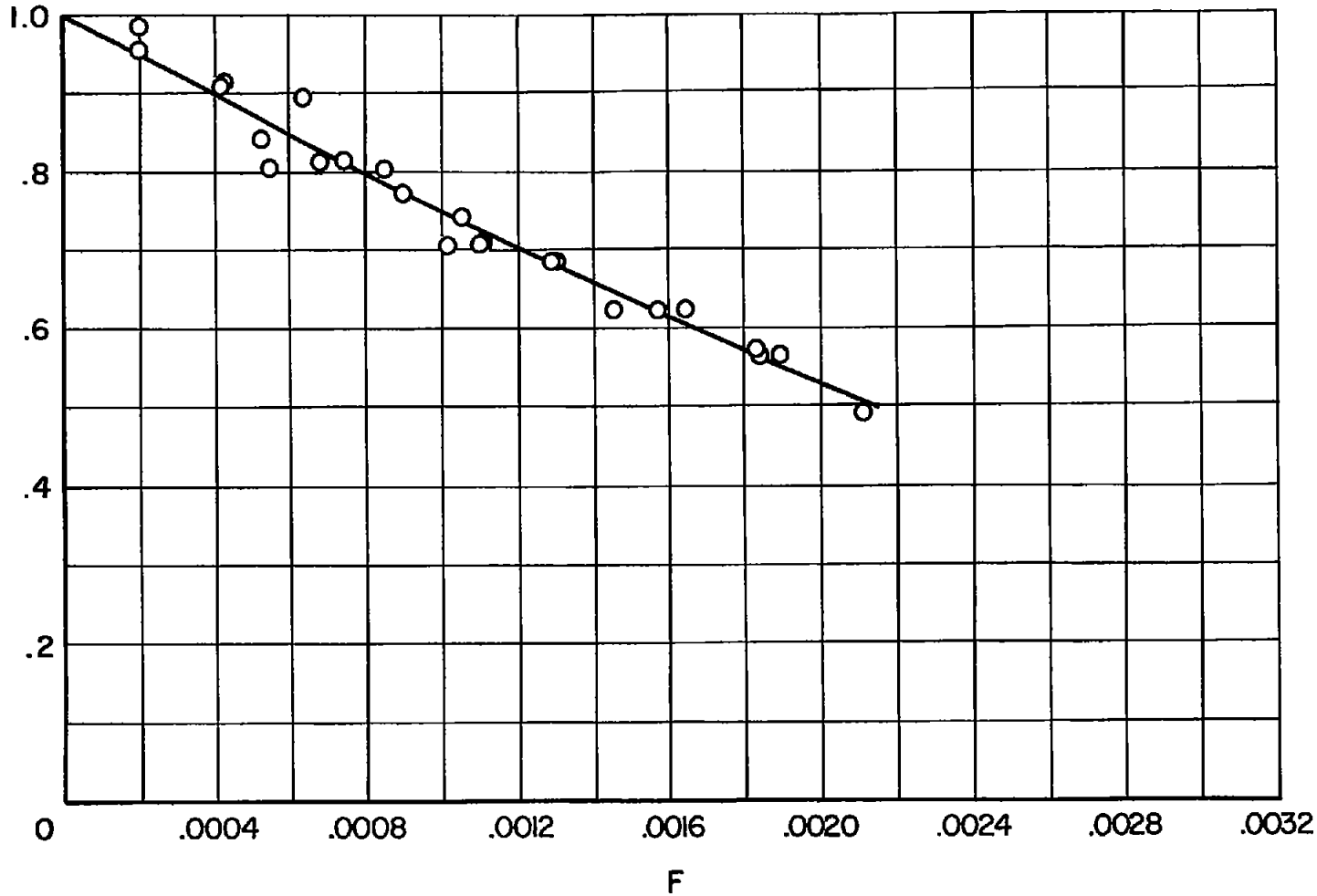

(a) R_∞ per foot = 6.25×10^6

Figure 4.- Variation of ratio of average skin-friction coefficient with transpiration rate.

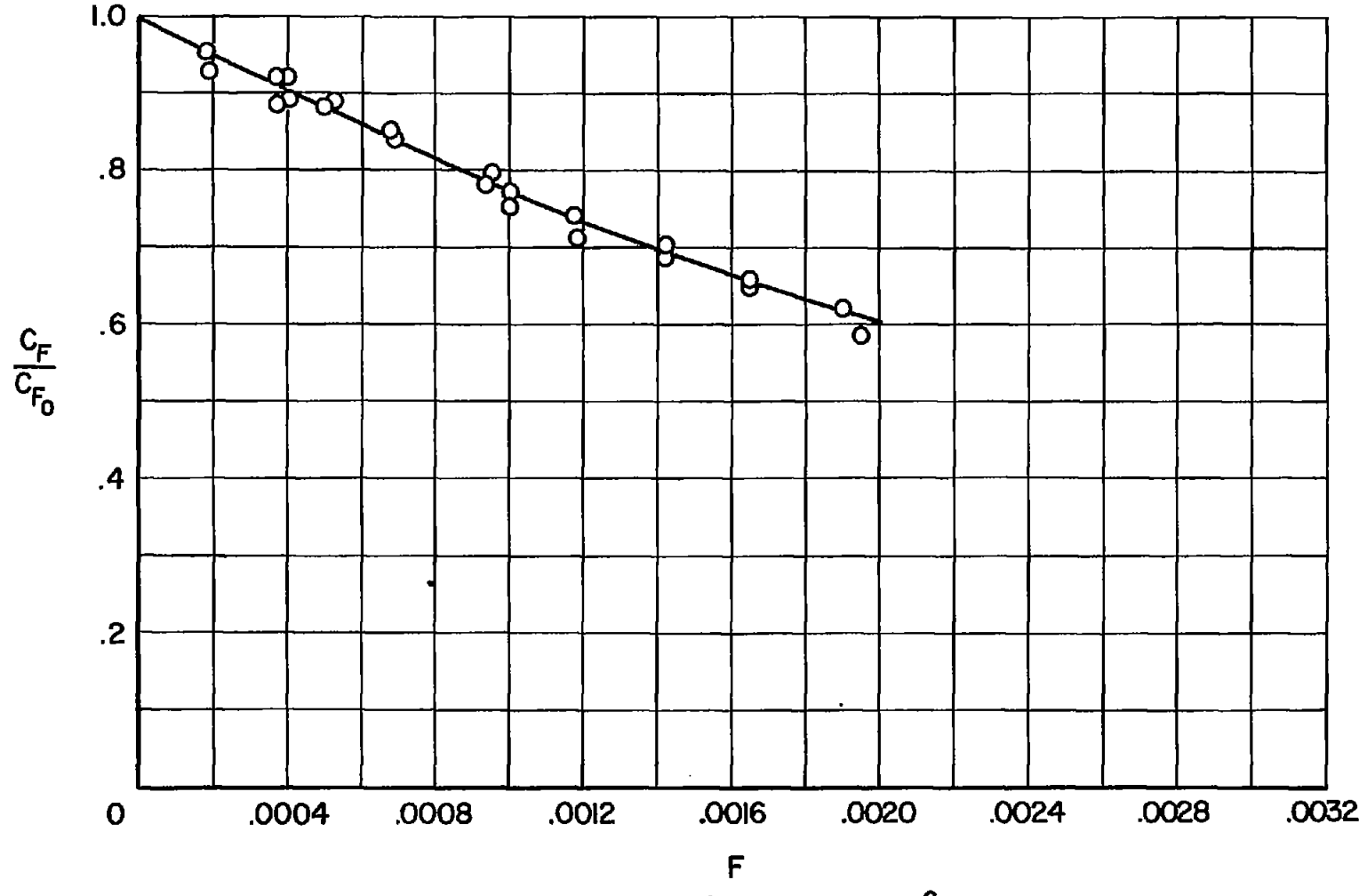

(b) R_∞ per foot = 6.94×10^6

Figure 4.- Continued.

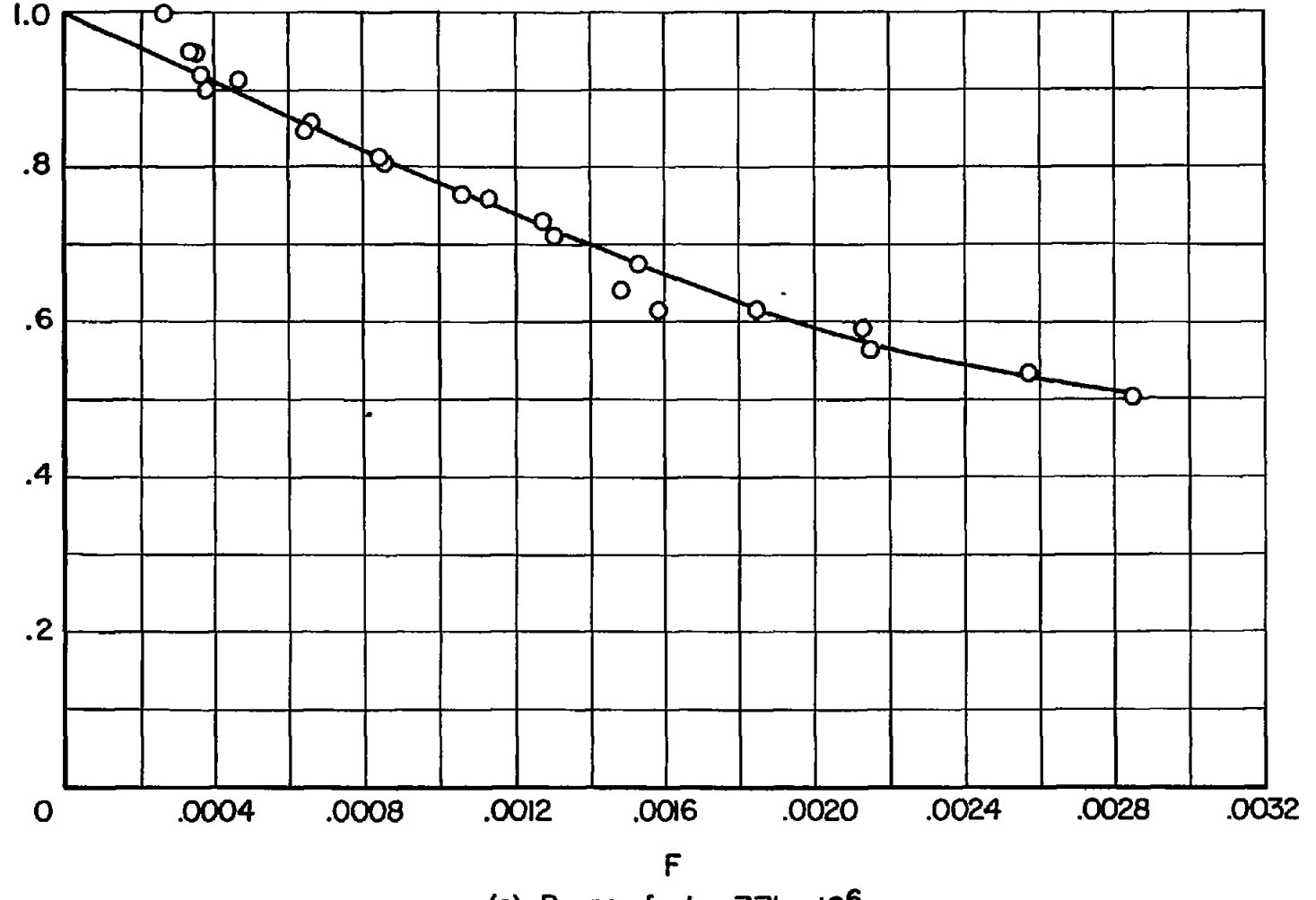

(c) R_∞ per foot = 7.71×10^6

Figure 4.- Continued.

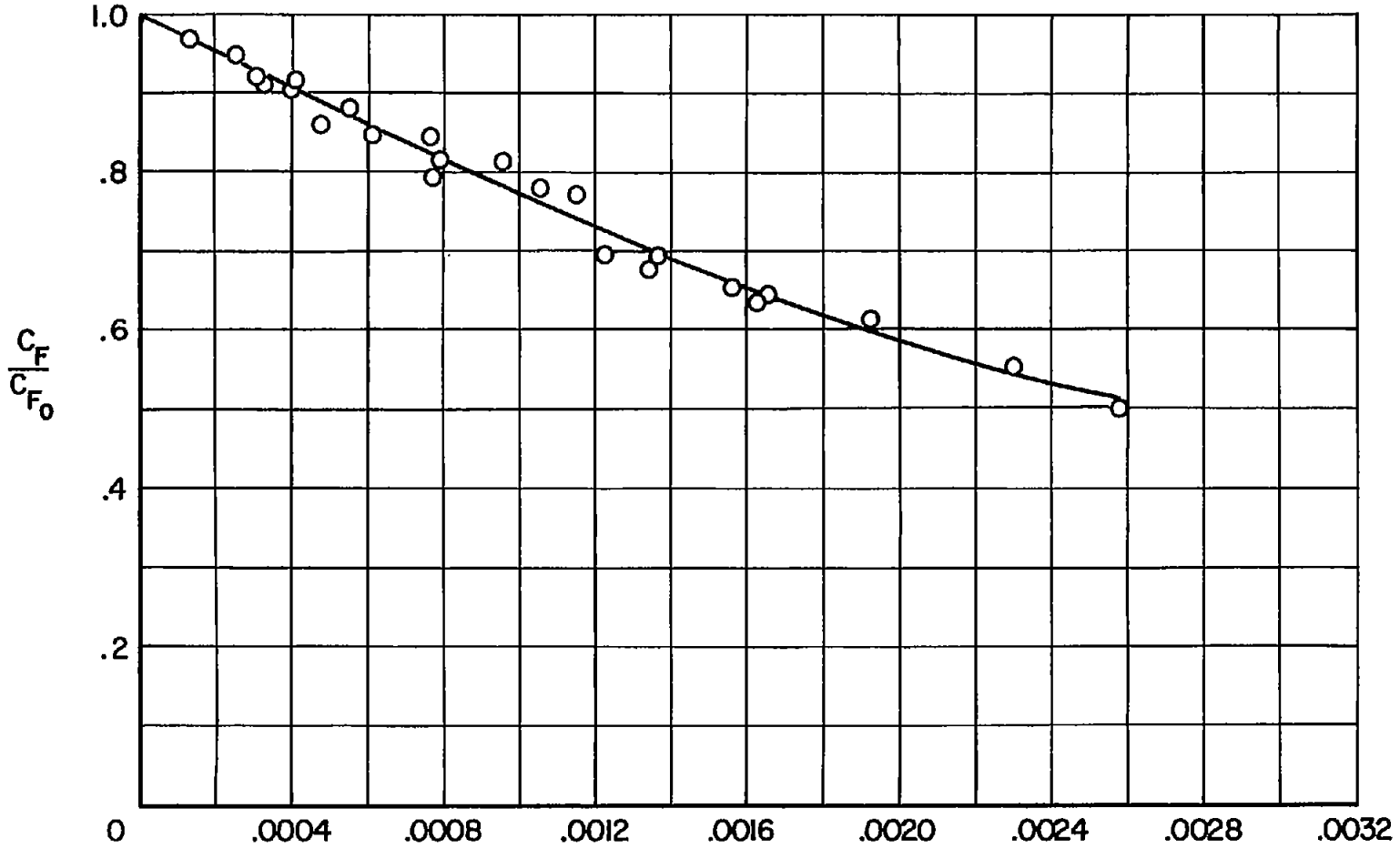

(d) R_∞ per foot = 8.56×10^6

Figure 4.- Concluded.

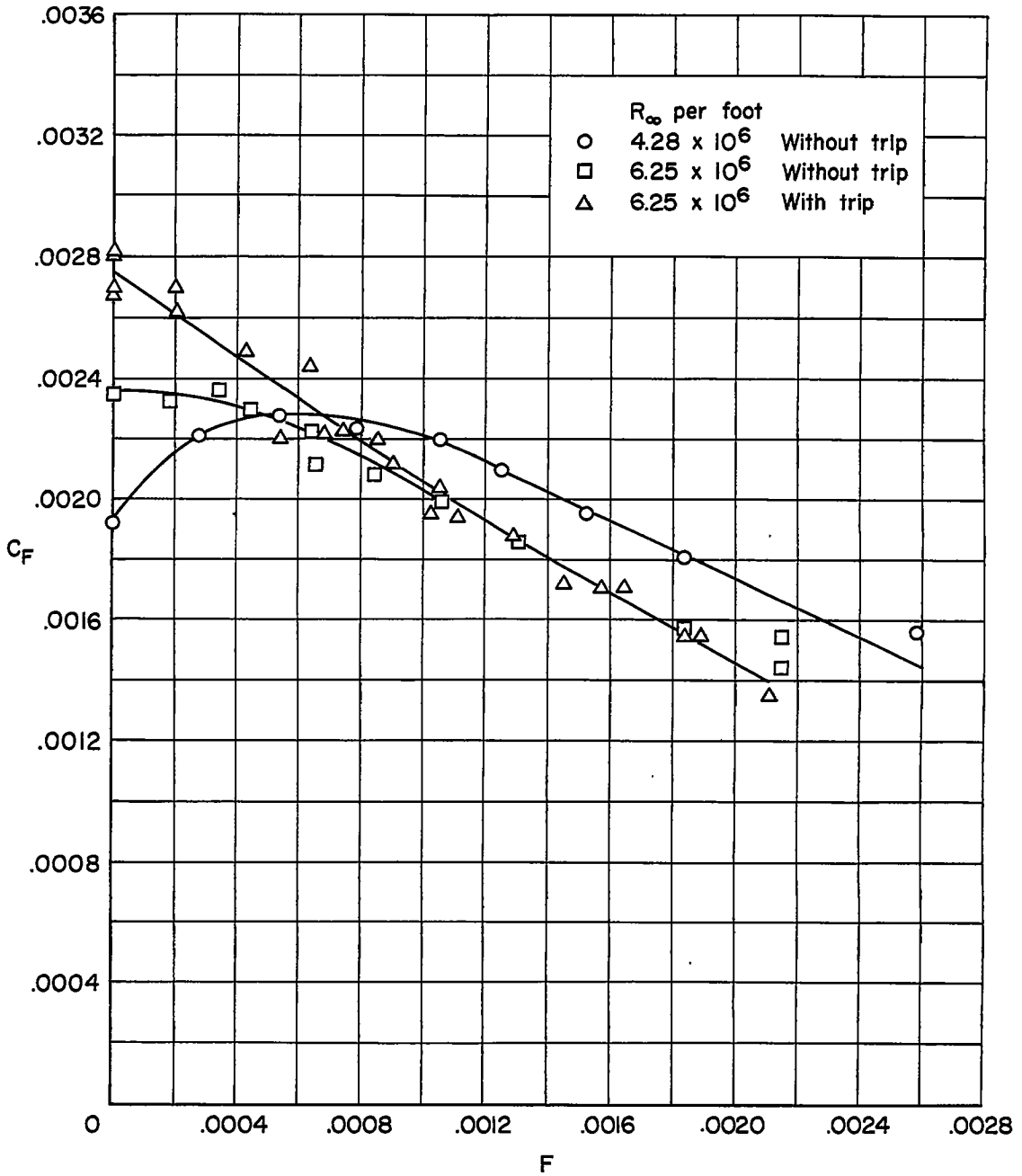

Figure 5.- The effects of a boundary-layer trip on average skin-friction coefficient at various transpiration air-flow rates.

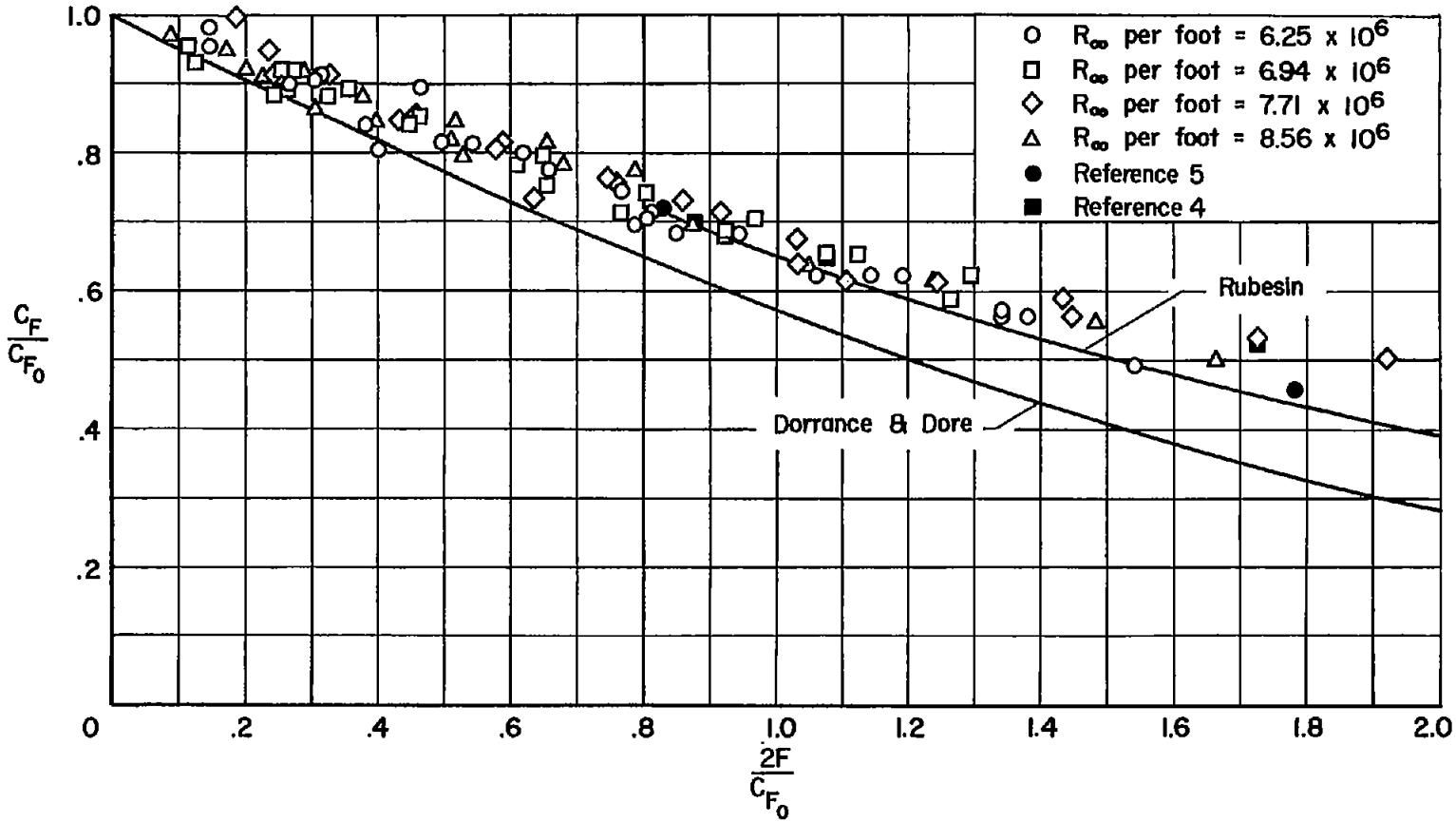

Figure 6.- Comparison of experimental data with theoretical predictions of the effects of transpiration air injection on skin-friction coefficients.